If "discrete breathers" is the answer, what is the question?

G. P. Tsironis[a)]
Department of Physics, University of Crete, P.O. Box 2208, Heraklion 71003, Crete, Greece

(Received 15 October 2002; accepted 13 January 2003; published 22 May 2003)

Intense work on discrete breathers or intrinsic localized modes in recent years has revealed a wealth of new properties of classical energy localization. Relaxation and mobility in particular may be two of the critical links with biomolecular processes. We review some of the basic discrete breather properties that we think are pertinent to biomolecules and make conjectures as to their possible biological utility. © *2003 American Institute of Physics.* [DOI: 10.1063/1.1557234]

Discrete breathers are nonlinear localized modes that can be created in translationally invariant nonlinear lattice models. Once generated, discrete breathers modify system properties such as lattice thermodynamics and introduce the possibility of nondispersive energy transport. We summarize these breather induced properties in nonlinear models and attempt to connect them with biological functions that could be assisted by the presence of breather modes in biomolecules.

I. INTRODUCTION

Recent progress in biological research at the molecular and atomic level provides science at large with a wealth of open problems that are both exciting and worthwhile to work on. Many of these problems hint to the fundamental complexity of systems and processes that seem to be the determining factor for the living matter. Biologically motivated physics[1] studies biological issues seen, however, with the eyes of physics where an explanation and understanding is tantamount to the formulation of a reasonably successful but fundamentally quantitative and simple model. Among the multitude of biological problems and puzzles that exist, many physicists in recent years became fascinated with protein folding[2] and energy and charge transport in biopolymers.[3] While protein folding seems at first hand to be a pure configurational problem, energy and charge transfer is a pure dynamical problem dealing with the modes that provide efficient and reliable operational capability in biological matter. In the present short exposition that is neither exhaustive nor reviews the existing literature, we will focus predominantly on the dynamical problem and attempt to piece together a handful of specific recent works on nonlinear localization that may be linked to biological research. Specifically, we will try to focus on the physical aspects of nonlinear localized modes that are known from work in simple models and that can be of use to dynamical processes in biopolymers. Clearly, even if physical aspects of these modes are interesting and *a priori* useful to biopolymers it does not follow that natural selection and evolution has actually chosen them for the biological processes. Before a definitive proof is available, their overall simplicity and thus Occam's razor can be our only additional argument.

In the literature one encounters terms such as polarons, solitons, breathers, ILM's, localons, etc., that are used many times interchangeably and in ways that lead to confusion; for simplicity and the purpose of the present article let us call all dynamical modes that are spatially localized as a result of some anharmonicity, nonlinear localized modes (NLM's). Nonlinear localized modes in the form of intrinsic localized modes (ILM's) or discrete breathers (DB's) that is our focus here are known only relatively recently while generally the concept of nonlinear localization in the form of solitons, self-trapped states or polarons is much older. Discrete breathers are NLM's that exist in lattices of nonlinear oscillators that are weakly coupled. They are dynamical modes that typically are time periodic and space localized in an exponential fashion. Some of their physical properties have been found in recent years, making them appealing energy agents in biopolymers and give some hints on their possible presence in these systems. In the present exposition we will review these properties of DB's and attempt to link them to biological matter and its properties. There is no proof at the present stage that DB's play any role whatsoever in biopolymers; there is, however, a growing body of primarily theoretical work that hints in this direction. We can only hope that actual proofs will be provided in the future. The structure of this article is the following: in the next section we form the physical basis for the biological utility of DB's based on relevant properties and in the remaining three sections we review these issues in more detail. Specifically, we look into the relaxation problem, the transport features of localized energy in curved chains and the focused transfer in the form of targeted transfer. In the last section we attempt to make a synthesis and provide a research outlook.

II. SUMMARY OF PHYSICAL PROPERTIES OF DISCRETE BREATHERS RELEVANT TO BIOMOLECULES

In this section we will enumerate known physical properties of DB's motivated by the following question: While it is clear that DB's exist in Hamiltonian lattices, are there any indications that may also be found in true complex biomolecules? Since experimental work usually gives indirect infor-

[a)]Also at the Institute of Electronic Structure and Laser, Foundation for Research and Technology-Hellas, P.O. Box 1527, 71110 Heraklion, Crete, Greece. Electronic mail: gts@physics.uoc.gr

mation and depends on specific properties, it might be more profitable to reverse the question and address it in the following way: *What are the DB properties that would in principle be useful in the organization of a complex biological micro-machine such as for instance a protein?* In order to address this question we need first to codify the known DB properties in simple lattices and subsequently extrapolate to more complicated systems. Although not exhaustive, the list of the following properties will be the basis for our passage from simple Hamiltonian models to complex biomolecules.

(i) **Existence and stability:** Although DB's were conjectured in several indirect forms, their initial explicit introduction was done by Sievers and Takeno in 1988 through an approximate method based on the rotating wave approximation (RWA) while subsequent work exemplified some of their properties.[4] In 1994 MacKay and Aubry proved a theorem that demonstrates the precise existence of DB's in a wide class of nonlinear lattice models.[5] It is now known that DB's not only exist rigorously in a large class of Hamiltonian systems but are also linearly stable. Although specifics vary depending on the system, discrete single and multi-breathers are formed typically in spectral regions that do not coincide with the linearized spectra of the lattices. They involve large amplitude collective oscillatory motion that engages only a local lattice neighborhood and whose influence decays exponentially in space. They thus represent system coherence or organization that is nevertheless of a very local nature.

(ii) **Nonexponential relaxation:** In the case of random DB generation, the lattice may form short-range order depending on the initial conditions. This order is made of various coherent DB regions separated by regions where only linear modes can be found. The DB's are then generally very robust and long-lived, although interaction among breathers is possible resulting in some cases in breather accumulation. If the system is placed in contact with a reservoir that absorbs energy, the lattice loses energy yet in a nonexponential fashion. This feature of slow relaxation is directly attributed to the presence of DB's.[6–10]

(iii) **Mobility:** Even though DB's are spatially quite discrete and may occupy very few sites, in many cases they move across the lattice with essentially ballistic, particle-like motion. This DB motion preserves their shape and frequency although in an approximate fashion. The speed of DB propagation is slower than the sound speed, i.e., the speed of the linearized phonon modes of the system. The DB motion can be induced through excitation of an appropriate linearized DB mode that enables DB depining and subsequent free propagation.[11–13]

(iv) **Targeted energy transfer:** When hard and soft nonlinear potentials are mixed in the lattice it is possible to have a nonlinear resonance that enables complete energy transfer from one oscillator to another. This phenomenon of targeted energy transfer (TET) is very selective and occurs only in a very narrow frequency region where the oscillators are spectrally entrained. The transfer between donor and acceptor sites in addition to being selective and efficient may occur in an irreversible fashion when the donor–acceptor pairs are coupled to a larger system that provides dephasing.[14,15]

The first property, that in addition to rigorous mathematical proofs, is also supported by numerous arithmetic investigations, warranties that DB's appear in nonlinear lattices in an almost generic fashion.[16,17] Although there are only few explicit indications yet that they also exist in more realistic lattice configurations, we believe that, based on the existing knowledge, we can safely conjecture that DB's exist in more complex models such as models for biopolymers.[18,19] As a result, we will make hereafter the reasonable assumption that property (i) holds for complex biopolymer models and we will accompany it with the operational conjecture that DB's can be in principle found in true biopolymers although without worrying yet about issues such as lifetime and function. In what follows, we will focus exclusively on the remaining three DB properties and will attempt to link them with biological activity. Specifically, property (ii) will be connected with multiple time scales and out of equilibrium relaxations while (iii) and (iv) to energy transfer processes.

III. STATISTICAL PROCESSES AND NON-EXPONENTIAL RELAXATION

When DB's are generated randomly in a nonlinear lattice,[20] they play the role of dynamical impurity modes characterized by a long but finite lifetime that depends both on the specific lattice and its temperature. To probe the role that DB's play in the macroscopic thermal features of the lattice, one may perform numerically transient experiments in the process of which DB's are generated, move as well as decay. If the lattice is coupled to a heat bath at temperature different than the lattice temperature, energy transfer occurs between the system and the bath. It was found in relaxation numerical experiments of this type with bath temperatures much smaller than lattice temperatures that spontaneously generated DB's can inhibit diffusive energy transfer and, as a result, the whole relaxation process is slow and in some cases it is described by a stretched exponential.[6,7] In what follows, we will describe a transient grating experiment that is similar to the transient relaxation experiment but it is performed in closed systems and, additionally, it is used for experimental diffusion constant determination. In thermal grating experiments[21,22] two time-coincident excitation pulses are crossed in the sample to produce an interference pattern. If the energy of the incident light coincides with that of an optical transition of the sample, the absorption mimics exactly the interference fringe and produces in the sample a diffraction grating in the form of excited states. At the end of the excitation pulse, the induced diffraction pattern starts to decay due to diffusion. This decay process is probed by a third beam that is temporally delayed and diffracted by the

induced grating. Finally, the measurement of the intensity of the diffracted probe beam with respect to the time delay allows to monitor the decay of the grating.

In transient gratings, the diffraction efficiency given by the ratio between the intensity of the incident probe and its diffracted beam is proportional to the modulus of the variation of the complex index of refraction, viz., proportional to $(\Delta k)^2+(\Delta n)^2$ where Δk and Δn refer to the peak-to-null difference in the imaginary and real part of the complex index of refraction that are induced by the interference pattern. The physical processes which contribute to the variation of index of refraction along the grating image are associated with the variation of the local population density of the absorption species as well as with the local lattice temperature modulation. The temperature related effects are produced after optically excited states rapidly release their energy to the lattice by means of photo-dark processes; this increases the phonon bath temperature and induces a diffraction heat pattern in the lattice. The evolution of the grating pattern thus follows the evolution of the lattice vibrations toward the equilibrium state which is accomplished through heat diffusion away from the peaks of the grating, corresponding to the highest lattice temperature, to its valleys. The grating signal is thus proportional to the square of the time dependent peak-to-null temperature difference ΔT of the grating pattern. In cases of standard diffusion, energy accumulated due to the initial peak-to-null temperature difference ΔT decays exponentially and from the measurement of the decay rate constant we may obtain the thermal diffusivity of the material. We demonstrate below that in models that support DB's, these features are true only in cases of low initial lattice excitation. Upon increasing the initial energy deposited in the lattice, the decay of the grating pattern starts deviating from the exponential decay and shows slow relaxation dynamics; as a result a macroscopic signature of DB presence is slow relaxation.

We consider a one-dimensional chain of atoms interacting through nearest neighbor linear interaction and experiencing a local on-site nonlinear potential $V(x)$:

$$H=\sum_n \left(\frac{p_n^2}{2}+V(u_n)+\frac{k}{2}(u_n-u_{n+1})^2\right), \tag{1}$$

where u_n, p_n are the position and momentum, respectively, of the nth oscillator. In order to have localized breather solutions, the strength of the coupling term in (1) has to be sufficiently small and the on-site contribution which is chosen to be the "hard" nonlinear potential $V(x)=Ax^2/2+Bx^4/4$ to be dominant.[5]

To simulate the thermal grating experiment we have to set an initial condition for the lattice variables p_n, u_n that mimics the thermal profile. To this purpose we chose the following initial configuration for the lattice temperature:

$$T_n=T_0[1+\cos(\pi+\eta(u_n-u^0))]/2, \tag{2}$$

where n denotes the lattice site, T_0 is the maximum temperature induced by the radiation field, $2\pi/\eta$ the wavelength of the diffraction pattern and u^0 the center oscillator of the chain. For the sake of simplicity, we assume that in the absence of a radiation field the lattice is at zero temperature. The initial conditions for the u_n, p_n are then chosen randomly according to a Gaussian distribution with position dependent temperature given by Eq. (2). We follow the time evolution of the normalized symmetric energy density, defined as $\epsilon_n(t)=[p_n^2/2+V(u_n)+(k/4)\{(u_n-u_{n+1})^2+(u_n-u_{n-1})^2\}]/\epsilon_{\text{total}}$ for each realization of the initial conditions in two different regimes: (a) small initial excitation of the lattice for the parameters used ($A=1,B=1,k=0.1$) corresponding to $T_0\ll 1$ with the nonlinearity of the potential not playing any role and (b) in the high excitation regime where breather-like hot spots appear that can trap the local excess energy for long time. The two different regimes show distinctly different relaxation properties that are manifested in the transient grating signal.

The grating signal $S(t)$ is proportional to the square of the peak-to-null difference of the temperature profile. This can be obtained by calculating the Fourier transform of the time dependent temperature profile at the wave length of the initial grating:[22]

$$f(t)=\sum_n e^{i\eta n}\epsilon_n(t), \tag{3}$$

$$S(t)=\left|\frac{f(t)}{f(0)}\right|^2.$$

In practice, for each initial realization of p_n, u_n, we calculate the energy profile and then we average this over the total number of realizations (a few thousand for a lattice of 73 oscillators and a grating wavelength extending over 16 lattice sites). Then we calculate the grating signal $S(t)$ using Eq. (3). From the numerical evaluation of $S(t)$ we find a regime dominated by the linear excitations of the lattice that do not interact among themselves and the decay of $S(t)$ is accompanied by an oscillatory behavior.[8,22] This feature is also seen in the energy landscape representation of Fig. 1(a). It is important to notice that, since in our model we did not introduce any dissipation mechanism, in the linear regime the decay of the signal is only due to dispersion effects [$f(t)$ is proportional to the energy Fourier transform of $\exp(i\epsilon(\omega)t)$ with $\epsilon(\omega)$ determining the phonon band]. However, it is clear that the unavoidable dissipation mechanisms present in the real system would transform this behavior in an exponential relaxation.[6] In the second temperature regime $T_0=0.5$ on the other hand, already for a short time, a different behavior is observed, both in the energy landscape [Fig. 1(b)] where the initially introduced heat patterns persist for long times as well as in the transient grating signal. In Fig. 2 we show the long-time evolution of $S(t)$ for several choices of T_0, ranging from intermediate to moderately strong values, and its corresponding log–log plots. We observe distinctly nonexponential relaxation induced by the very slow dynamics induced by the breather segments and associated with the trapping of thermal energy.[8]

Given an arbitrary initial condition for the lattice variable with temperature profile (2), the breather modes will be most likely located at the highest peaks of the profile. As a consequence, since the energy carried by these local excitations is trapped for long time, the grating profile maintains its shape for a long time and this is reflected in the slow non-

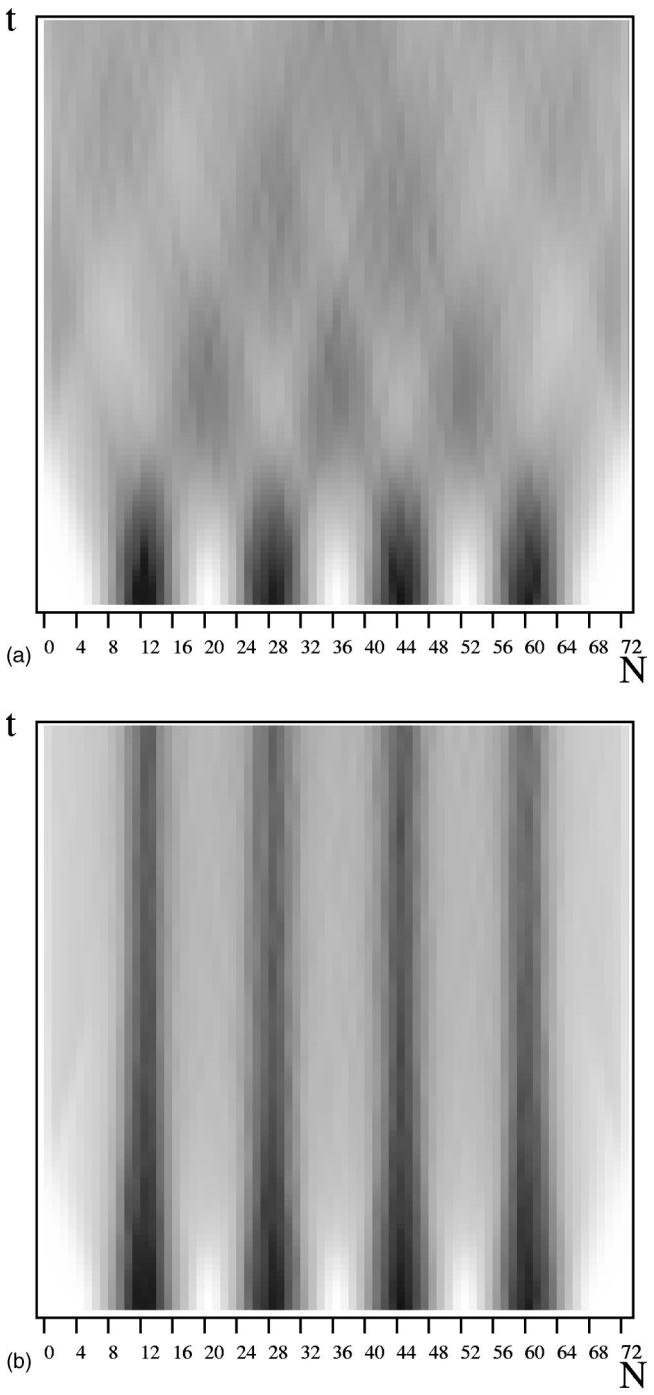

FIG. 1. Evolution of the averaged symmetrized energy landscape corresponding to (a) $T_0=0.05$ and (b) $T_0=0.5$. Dark regions correspond to highs in local energy accumulation. In the horizontal axis we have the lattice sites whereas in the vertical local energy density snapshots as a function of time. We show the averaged results over an ensemble of few thousand random initial realizations, with a time unit equal to 100 periods of the linearized oscillations and $\eta=2\pi/16$.

exponential decay process of the grating signal. The specific functional form for the decay function is not essential; what is important is the fact that the presence of NLM's such as breathers induce slow relaxation.[10] The time persistent feature of the breather induced pattern eventually disperses in a closed system.

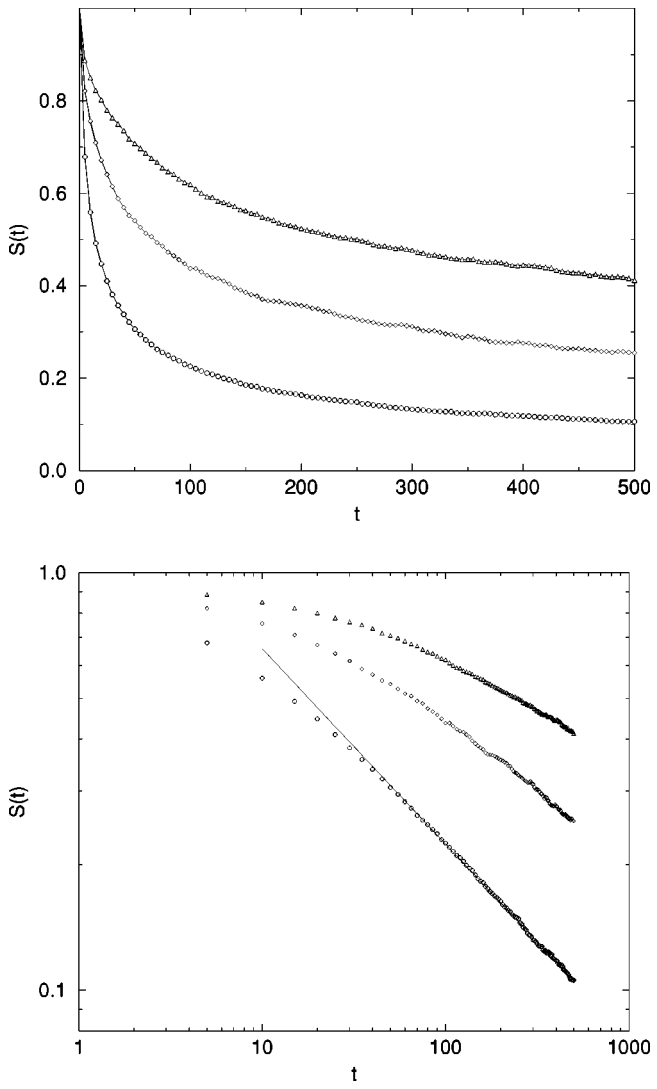

FIG. 2. The relatively long time evolution of the grating signal $S(t)$ for intermediate to relatively strong values of the initial grating amplitude T_0. In the upper panel: the lowest curve corresponds to $T_0=0.4$, the intermediate to $T_0=0.6$ and the highest to $T_0=0.8$. In the lower panel: the log–log plot of the preceding case. The full line is a power law relaxation fit corresponding to $S(t)=1.93t^{-0.468}$. The same system parameters as in the previous figure.

IV. ENERGY PROPAGATION IN CURVED CHAINS

In order to address property (iii) we will focus on polymeric-like chains of masses coupled with springs that can move in the whole (x,y) plane and are characterized by local and global elastic properties. Since our main interest is in understanding the physics of breathers in biomolecules such as proteins[1] rather than general homopolymers, we will have to somehow restrict our study to rigid and quasi-rigid polymer geometries. This can only be done artificially through constraints when only first neighbor interactions are taken into account due to the high level of degeneracy of the chain. We will report on the issue as to whether a stable breather can be generated in a curved polymer with some rigidity, if it can propagate in this polymer as well as hint on the features of its motion and the feedback of localized energy in the elasticity of the polymer.[23–25]

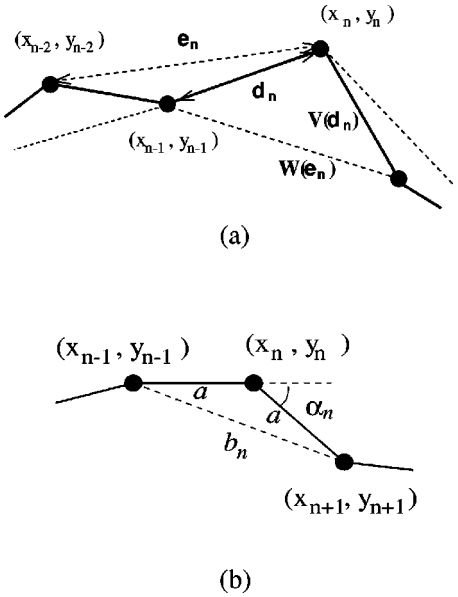

FIG. 3. (a) A picture of the model. The interaction between nearest neighbors is controlled by potential $V(d_n)$ and depends on their relative distance d_n (full lines). There is also an interaction between second neighbors controlled by $W(e_n)$, which depends on their relative distance e_n (broken lines). (b) Equilibrium distances $a_n=a$ and b_n between adjacent masses and next nearest neighbors, respectively, as a function of the relative angle α_n.

Let us consider a curvilinear polymer chain such as the one depicted in Fig. 1(a). The chain consists of N molecular units interacting through pair-wise two body interactions, assuming that (a) all unit masses are identical and equal to m, (b) there are only first and second neighbor interactions between the molecular units and (c) the polymer lies on the (x,y) plane.

Each mass unit in the chain is labeled by an index n, while its location is specified through the pair (x_n,y_n) denoting its location on the plane with respect to an absolute Cartesian system. Since we will use first and second neighbor interaction potentials we need to introduce the following two Euclidean distances:

$$d_n=[(x_n-x_{n-1})^2+(y_n-y_{n-1})^2]^{1/2}, \tag{4}$$

$$e_n=[(x_n-x_{n-2})^2+(y_n-y_{n-2})^2]^{1/2}. \tag{5}$$

We note that d_n, e_n are simply the distances on the plane between the nth unit and the $n-1$th and $n-2$th units, respectively. The polymer chain plasticity as well as rigidity is controlled by the ensemble of first and second neighbor constant equilibrium distances $\{a_n\}$ and $\{b_n\}$, respectively. The constant a_n is the equilibrium oscillator distance between units n and $n-1$ while b_n is that between the nth and $n-2$th units. The explicit configuration of these two set of constants fixes the desired equilibrium geometry of the polymer chain. Although the derivation presented here is general, we are mostly interested in the case $a_n=a$ for all n with b_n depending on the geometrical structure we want to study, i.e., it fixes the relative angles α_n [see Fig. 3(b)]. For the interaction we use Fermi–Pasta–Ulam (FPU) type potentials:

$$V(d_n)=K_1\frac{(d_n-a_n)^2}{2}+\beta_1\frac{(d_n-a_n)^4}{4}, \tag{6}$$

$$W(e_n)=K_2\frac{(e_n-b_n)^2}{2}+\beta_2\frac{(e_n-b_n)^4}{4}. \tag{7}$$

The Hamiltonian for the planar polymer chain can be then written as

$$H=\sum_n \frac{m}{2}(\dot{x}_n^2+\dot{y}_n^2)+\sum_n \{V(d_n)+W(e_n)\}, \tag{8}$$

where the index n runs over all polymer masses. The resulting equations of motion are

$$m\ddot{x}_n=-\frac{\partial}{\partial x_n}U_n, \quad m\ddot{y}_n=-\frac{\partial}{\partial y_n}U_n, \tag{9}$$

with

$$U_n=V(d_n)+V(d_{n+1})+W(e_n)+W(e_{n+2}). \tag{10}$$

Using normalized relative variables $\xi_n\equiv(x_n-x_{n-1})/a$ and $\rho_n\equiv(y_n-y_{n-1})/a$ where a is a length scale, we rewrite the Euclidean distances as $d_n=a^2[\xi_n^2+\rho_n^2]^{1/2}$ and $e_n=a^2[(\xi_n+\xi_{n-1})^2+(\rho_n+\rho_{n-1})^2]^{1/2}$, respectively, and upon the introduction of the complex coordinate $z_n=\xi_n+i\rho_n$ we obtain the following compact form for the equations of motion:

$$\ddot{z}_n=R_{n+1}+R_{n-1}-2R_n+Q_{n+2}-Q_{n-1}-Q_n+Q_{n-1}, \tag{11}$$

where for the specific FPU potentials of Eqs. (6), (7) we have

$$R_n=\frac{z_n}{|z_n|}[(|z_n|-\tilde{a}_n)+\gamma_1(|z_n|-\tilde{a}_n)^3], \tag{12}$$

$$Q_n=\frac{z_n+z_{n-1}}{|z_n+z_{n-1}|}[\lambda(|z_n+z_{n-1}|-\tilde{b}_n)+\gamma_2(|z_n+z_{n-1}|-\tilde{b}_n)^3], \tag{13}$$

where time has been put in dimensions as $t\to t\sqrt{K_1}$ and the parameters are $\gamma_1=a^2\beta_1/(mK_1)$, $\lambda=K_2/(mK_1)$, $\gamma_2=a^2\beta_2/(mK_1)$, $\tilde{a}_n=a_n/a$ and $\tilde{b}_n=b_n/a$.

In order to specialize to a model with only first-neighbor interactions but with some form of rigidity we constrain the relative angles between adjacent bonds to constant but arbitrary values by writing Eq. (11) with only first neighbor interactions, using the polar representation $z_n=r_n\exp(i\theta_n)$ and introduce additionally the local relative displacement $\tau_n\equiv r_n-\tilde{a}_n$. The constraint of fixed relative angles in these new variables reads as $\ddot{\theta}_n=\dot{\theta}_n=0$, $\theta_n(t)=\theta_n(0)$. After some algebra[24] we obtain a reduced dynamical model described by the equations

$$\ddot{\tau}_n=\epsilon_{n+1,n}\hat{f}_{n+1}+\epsilon_{n,n-1}\hat{f}_{n-1}-2\hat{f}_n,$$
$$\epsilon_{n,n-1}=\cos(\theta_n-\theta_{n-1}), \tag{14}$$
$$\hat{f}_n=-f_n,$$

with a force $\hat{f}_n$ that, in the specific case of the FPU potential of Eq. (6), is simply

$$\hat{f}_n=\tau_n+\gamma_1\tau_n^3. \tag{15}$$

We term Eqs. (14) and (15) a modified Fermi–Pasta–Ulam equation (mFPU). For a straight line geometry, $\theta_n=\theta^0$ for all

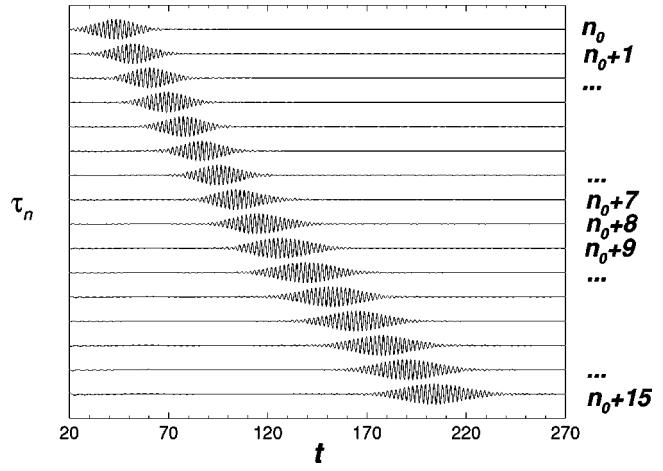

FIG. 4. The DB amplitude τ_n as the DB's moves along a straight line and enters into a curved region, which starts at site n_0+8. As all τ_n oscillate around zero, we have displaced them by $\tau_n=\tau_n+nC$ where $C=0.4$. The characteristic angle of the hairpin is $\alpha=\pi/25$.

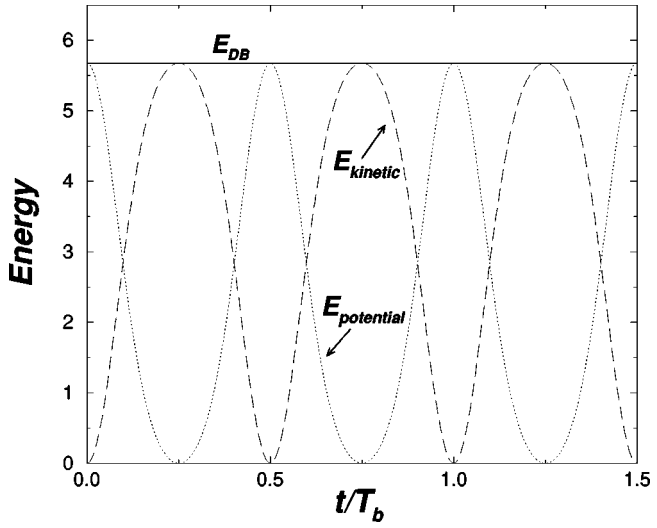

FIG. 5. Energy of a *static* DB with $T_b=2.122$ in a straight line (FPU model).

n, the mFPU is equivalent to the FPU model ($\epsilon_{n+1,n}=1$), which can be obtained from Hamiltonian (8) in a one-dimensional space. To mimic a β-sheet we choose the two-dimensional shape of a hairpin consisted of two parallel straight segments joined together from one side by a semi-circular arc.[24,25] We integrate numerically the mFPU model and obtain DB properties. Static DB's can be easily obtained corresponding to any desired geometry, circular or zig–zag; these DB's are rendered mobile in the straight sections of the hairpin.[24] From the study of the DB center of mass dynamics we find that a DB traverses a curved region or re-bounces depending on its initial velocity and on the local curvature. For a given hairpin geometry, the DB re-bounces for small velocities, while for higher velocities it traverses the curved region. For a given initial velocity in the straight region, the DB re-bounces or enters into the curved region depending on α. There is a critical curvature below which the DB is able to pass and above which the DB is reflected. In some cases, for critical velocities or critical angles α, the DB is trapped in the bend. When re-bouncing, the DB velocity remains unchanged. In contrast, when traversing the curved region, the DB velocity decreases but once the DB reaches the other straight segment it recovers the initial velocity. The amplitude of the local site oscillations as the DB enters from the straight to the bend section as a function of time is plotted in Fig. 4; we note simply differences in the oscillation duration resulting form the smaller DB velocity in the bend region.

In the hairpin, DB's either propagate through the bend or get reflected while they principally keep their identity and basic features; the specifics of this dynamics are controlled by a local DB energy conservation. The energy of a nonmoving breather on the DB energy alternates between all potential and all kinetic. If through E_{DB} we denote the internal breather energy we observe (Fig. 5) that is to high accuracy ($\sim 10^{-8}$) constant. The total energy for a nonmoving breather is thus

$$E_{\mathrm{DB}}=E_{\mathrm{pot}}+E_{\mathrm{kin}}. \tag{16}$$

For a mobile breather we select a moving lattice window centered on the central DB site. The local energy exchange between kinetic and potential energy seemingly proceeds in a fashion similar to the one of the static DB. Nevertheless, some small in magnitude but clearly discernible differences emerge, as is seen in the inset of Fig. 6, that magnifies a selected segment; this difference corresponds to the translational energy of the mobile breather. Designating by ΔE_1, ΔE_2 the differences, respectively, of the maximum potential and kinetic breather energies from the total DB energy, E_{DB} we approximate the translational DB energy by

$$E_{\mathrm{tr}}=E_{\mathrm{kin}}^{\max}-E_{\mathrm{pot}}^{\max}\equiv\Delta E_1-\Delta E_2. \tag{17}$$

As seen in the inset of Fig. 6, the translational DB energy E_{trans} is only a small fraction of its total energy E_{DB} (E_{trans} is at most 1% of E_{DB} but typically much smaller); the measured

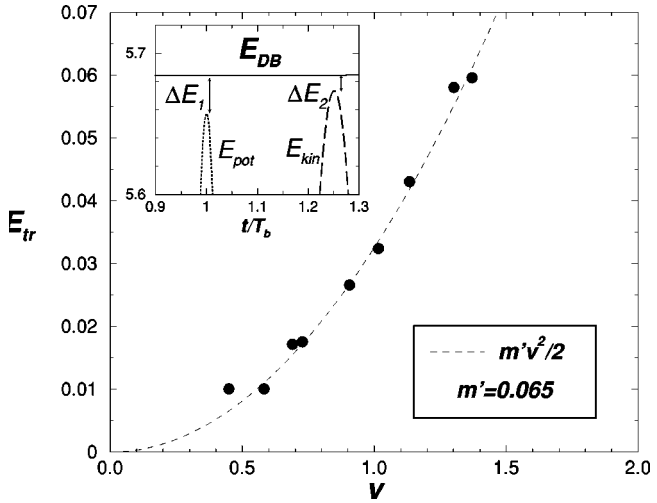

FIG. 6. Translational energy of a mobile DB in a straight line (FPU model) as a function the velocity. The sound velocity here is 10. The dashed line is a parabolic fit, corresponding to $v_{\min}=0$. Inset: Amplification of the energies of a *mobile* DB with $T_b=2.122$ and $v_0=0.1545$ in a straight line (FPU model).

translational energy as a function of the DB velocity is plotted in Fig. 6. By fitting the translational energy as a kinetic energy of a compound object, we obtain an effective breather mass that turns out to be much smaller than the individual particle mass.

In order to explore the influence of the curved region in the total energy of the DB, we calculate the breather energy after crossing the curved region. Before entering into the curved region and after exiting, the DB energy decays exponentially with a very slow decay rate of order $\sim 10^{-6}$, due to the nonexact character of the mobile DB. There is no extra loss of energy just after exiting compared to just before entering. Therefore we can consider that there are no appreciable energy losses as a result of motion in the curved part of the chain, and thus roughly speaking we can stay that DB motion in curved chains conserves the breather energy.

While retaining the rigidity around a predesigned line we lift the angular restriction imposed upon the local polymer angles in by including first and second neighbor interactions in the model.[25] Both first and second neighbor interactions are taken to be similar but with different coefficients, i.e., symmetric quartic polynomials in the relative displacements between masses with different quadratic and quartic strengths. Rigidity to a line on the plane is accomplished in this case through the second neighbor interaction coefficients b_n that vary locally in such a way so that a desired geometry in the equilibrium chain structure is produced, as can be seen in Fig. 3(b). The nearest neighbor nonlinear interaction is mostly responsible for the local longitudinal dynamics whereas the next nearest neighbor interaction for the geometric and angular rigidity of the chain. We use hairpin geometry and launch a longitudinally exact breather. The features of the motion are generally similar to the ones with only first neighbor interactions, viz., DB survival and propagation through the hairpin or re-bouncing accompanied, however, with small but constant energy loss. This loss depends on the specific parameter regime but generally does not lead to breather destruction. One new feature compared to the mFPU model is the DB propagation with a preferred velocity that is reached regardless of the initial DB velocity, i.e., either by deceleration or acceleration.[25] In the more realistic case of first and second-neighbor interactions we find that DB motion in the polymeric chains contains two seemingly general features, i.e., that geometry induces an energy loss to the breather and also a selection mechanism for an optimal propagation velocity. The energy loss is clearly induced initially at the bend region but it is preserved at much slower rates even when the breather returns in a rectilinear geometry. The terminal velocity, on the other hand, does not seem to be very sensitive on the specifics of the chain or the geometry of the bend. These DB properties arise from the additional translational and rotational flexibility that the chain has now and the intricate feedback mechanism between the longitudinal and transversal degrees of freedom. This results in a more efficient DB energetic adaption to the local environment while the increase (or decrease) in speed can be linked to a resonant energy exchange between transverse and longitudinal internal modes of the breather and channeling of some additional energy into the translational degrees of freedom. As a result of these properties, the DB emerges as an efficient energy transfer agent in more complex geometries that can be generated locally and transfer energy in an adoptive fashion engaging the local geometry to its dynamical state.

V. FOCUSED TRANSFER

Property (iv) is related to the specificity of energy transfer in biomolecules. While properties (i)–(iii) demonstrate that DB's can be used in principle in a biomolecular environment as energy agents, they cannot explain the specificity of transfer that occurs in several occasions. Examples of this type of focused energy transfer can be found in photosynthesis[26] where light harvesting occurs through photon capture by the antenna-like function of the photosynthetic unit. Energy self-focusing takes place as an electronic vibration (exciton) on a single pigment-protein and from there it is transported coherently through a complex cascade of transfer within and in-between pigment proteins. Then, it reaches the photosynthetic reaction center of the photosynthetic unit where it is converted into ATP. Another interesting example of focused transport can be found in biological motors where localized energy deposition through, for example, ATP hydrolysis is transferred almost losslessly over a relatively large distance at specific molecular locations enabling conformational biomolecular changes and conversion into mechanical energy.[27–31] Focused resonant transfer is possible in discrete nonlinear lattices in the form of targeted energy transfer (TET),[14,15] and we think that this very selective transport mechanism may be functional in true biopolymers as well.

The process of TET depends on a highly selective nonlinear resonance and it can be easily explained in the context of the discrete nonlinear Schrödinger (DNLS) equation:

$$i\dot{\psi}_n = \epsilon_n \psi_n + \lambda(\psi_{n+1} + \psi_{n-1}) - \chi_n |\psi_n|^2 \psi_n, \tag{18}$$

where ψ_n is the complex density amplitude at site n, ϵ_n represents the local site energy or frequency at the same site, λ controls the transfer to adjacent sites while χ_n is the site-dependent nonlinearity parameter. We will focus in the case of a system with only two sites, the first one corresponding to a donor (D) molecule while the second being the acceptor (A) and analyze the energy transfer features from D to A. Let us consider first the standard case where $\chi_1 = \chi_2 \equiv \chi$ and $\epsilon_1 = 0$ while $\epsilon_2 = \epsilon$:

$$i\dot{\psi}_1 = \lambda \psi_2 - \chi |\psi_1| \psi_1, \tag{19}$$

$$i\dot{\psi}_2 = \lambda \psi_1 - \epsilon \psi_2 - \chi |\psi_2| \psi_2. \tag{20}$$

Upon introduction of the variable p equal to the population density difference between the two sites where $p = |c_1|^2 - |c_2|^2$ as well as some manipulations, we obtain an effective equation for the density difference p:

$$\ddot{p} + W(p) = 0, \tag{21}$$

where $W(p)$ is a quartic polynomial of some general form.[32] The form of the equation denotes that transfer can take place between D and A but with rates that depend on the nonlinearity parameter.

In the degenerate case[33,34] as well as the nondegenerate case[32] complete energy transfer occurs for couplings λ larger than some critical one, while for smaller λ-values incomplete transfer occurs. However, in all cases the transfer period is substantially elongated as a result of the presence of nonlinearity and coupling. In the complete degenerate nonlinear dimer case, the oscillation period is $T=2\pi\mathbf{K}[\chi/(2\lambda)]$, where **K** is the complete elliptic integral of the second kind. While the transfer is slow and highly inefficient in this case, the fact that the resonant donor–acceptor pair is always at resonance, makes this nonlinear configuration the most efficient one with regard to energy transfer. To obtain the TET case we use a D–A dimer with $\chi_1=-\chi_2\equiv\chi$ and $\epsilon_1=0$ while $\epsilon_2=-\epsilon$:

$$i\dot{\psi}_1=\lambda\psi_2-\chi|\psi_1|\psi_1, \tag{22}$$

$$i\dot{\psi}_2=\lambda\psi_1-\epsilon\psi_2+\chi|\psi_2|\psi_2. \tag{23}$$

Upon transforming in the p-variable equation we get

$$\ddot{p}+[(2\lambda)^2+(\epsilon-\chi)]p=2\lambda(\epsilon-\chi)r_0+(\epsilon-\chi)^2p_0, \tag{24}$$

where r_0 and p_0 are initial conditions.[32,34] We note that nonlinearity has been effectively eliminated; furthermore, for perfect initial energy localization in the donor molecule ($r_0=0$ and $p_0=1$) *and* under the condition $\epsilon\equiv\chi$ we have perfect resonance determined through the equation

$$\ddot{p}+[(2\lambda)^2]p=0. \tag{25}$$

This precise resonance in the DNLS TET is linked to the equation normalization that may be taken unity, viz., $|\psi_1|^2+|\psi_2|^2=1$. Considering the nonlinear TET dimer as an effective tight-binding dimer, we find that the *effective local energies* of the latter, viz., $\epsilon_1^{\text{eff}}=-\chi|\psi_1|^2$ and $\epsilon_2^{\text{eff}}=-\chi+\chi|\psi_2|^2=-\chi[1-|\psi_2|^2]=-\chi|\psi_1|^2$ are equal at all times thereby allowing permanent resonance with perfect, reversible transfer. We find that by starting from the initial state state $\psi_1(0)=1$, $\psi_2(0)=0$, the energy oscillates between donor and acceptor with the largest possible frequency 2λ. After time $T=\pi/(2\lambda)$, the energy is completely transferred from the donor to the acceptor site while in the end of the next half period the energy returns fully to the donor oscillator. A departure from the exact targeting condition, either through ''errors'' in the initial conditions or the precise TET constraints leads to transfer with reduced efficiency, i.e., the oscillation period becomes much larger while less transfer is actually taking place. The proximity to the nonlinear resonance is controlled by a detuning function.[15]

In a real physical or biological system the donor–acceptor pair will be interacting with additional degrees of freedom. A direct consequence of this interaction is that the targeted transfer acquires unidirectional character. While the exact resonance condition is kept, most donor energy is transferred completely to the acceptor; however, as a result of the environmental interactions, the resonant condition is broken, making it impossible for a complete energy return to the donor site. As a result, true targeting occurs allowing for complete nonrecurrent energy transfer. The situation depicted in Fig. 7 represents such a case whereby the donor–acceptor pair is embedded in a long chain of linear oscillators coupled through a nearest-neighbor coupling constant λ. The initial condition $\psi_1(0)=1$ (donor site) and $\psi_i(0)=0$ for $i\neq1$ is the precise resonant condition for targeted transfer from the donor to the acceptor (site 2). Indeed, such transfer occurs very efficiently, but subsequently, as a result of the interaction with the rest of the chain, most energy remains localized on the acceptor site without returning to the original site. The presence thus of the ensemble of alternative sites introduces dephasing and, as a result, reversibility in the transfer.

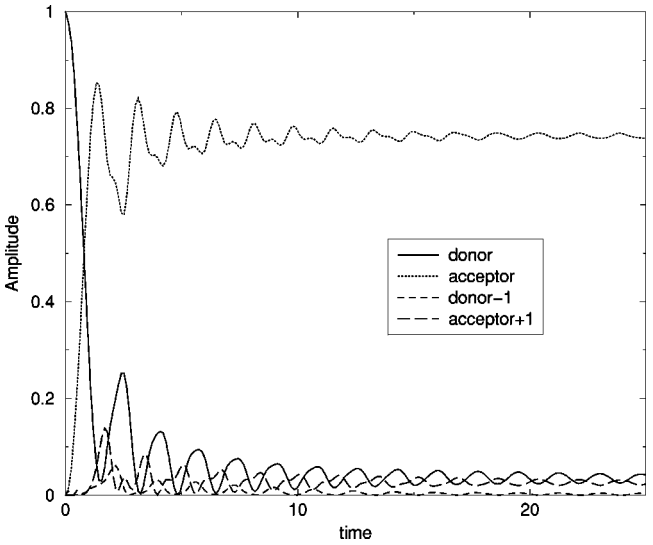

FIG. 7. A single donor–acceptor resonant pair embedded in a linear oscillator chain. The value of $\lambda=0.05$ and the amplitude is normalized to unity. We plot the amplitudes $|\psi_i|^2$ at the donor and acceptor sites, as well as the sites adjacent to them in a linear chain of over 10^3 sites. For the specific choice of λ, fast and efficient targeted transfer occurs over 70% of the initial energy.

There are numerous cases in biological materials where energy transfer occurs over several lattice sites in a seemingly coherent fashion. To test whether the TET could function over longer distances we embed a resonant nonlinear pair in a lattice of coupled linear oscillators but separate the nonlinear donor from the acceptor through N intermediate sites. We note that no special care was taken here in deriving a precise modified resonance TET condition in the presence of the new states; as a result we do not expect perfect resonant transfer.

The results of this experiment are presented in Fig. 8, where we observe energy propagation through the N site intermediate segment and intermittent capture by the acceptor site with transfer efficiency around 30%, depending on N, λ and the initial state. We note that in a perfectly linear system the corresponding transfer would be practically zero except for a transient.

Under the TET resonance condition coherent energy transfer can take place between donor and acceptor sites of a nonlinear network. This targeted transfer is periodic in a dimer system but becomes unidirectional when environmental interactions are taken into account, as in the case of Fig. 8. Under appropriate conditions it can take place over larger distances, leading to the possibility of use in bioenergetics and materials science. In Figs. 9 and 10 we show two cases

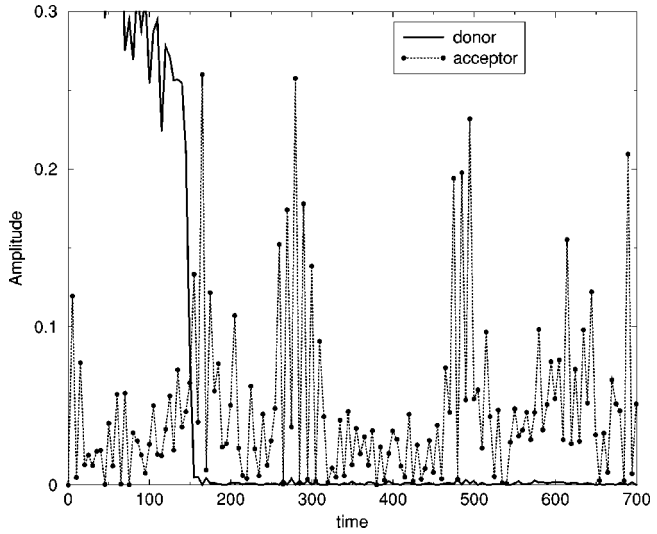

FIG. 8. A resonant donor–acceptor pair embedded in a linear oscillator chain and separated by $N=8$ linear oscillators having the same linear potential as the acceptor site. The value of $\lambda=0.125$ and the amplitude is normalized to unity. We plot the amplitudes $|\psi_i|^2$ at the donor and acceptor sites. In order to satisfy the resonant condition, all amplitude is located initially at the donor site. We observe substantial transfer in the acceptor site while some intermittency is present due to the exact Hamiltonian nature of the system. In the linear or fully nonlinear cases the transfer over ten sites in a chain with over 10^3 oscillators would be practically zero.

of TET transfer over longer distances; while no special care was taken in modifying appropriately the TET condition[15] by taking the intermediate oscillators into account, we see that selectivity between the separated D–A pairs is evident.

This feature could have resulted through an adaptive evolutionary process in some biologically interesting cases but could also be used for the design of complex materials with prescribed energy transfer properties. What is important for targeted transfer is the tuning of nonlinearity and the initial conditions of different, distant oscillators. Several factors that have not considered explicitly yet, such as noise, disorder and nonlinearity of the environmental degrees of freedom, might in some cases, enhance the long-distance targeting effect. Noise, for instance, can provide an adequate mismatch in order to render the energy transfer completely irreversible while the transfer might not be affected substantially by static disorder. The interaction with additional degrees of freedom leading to polaronic or other effects can have also an effect in the transfer.

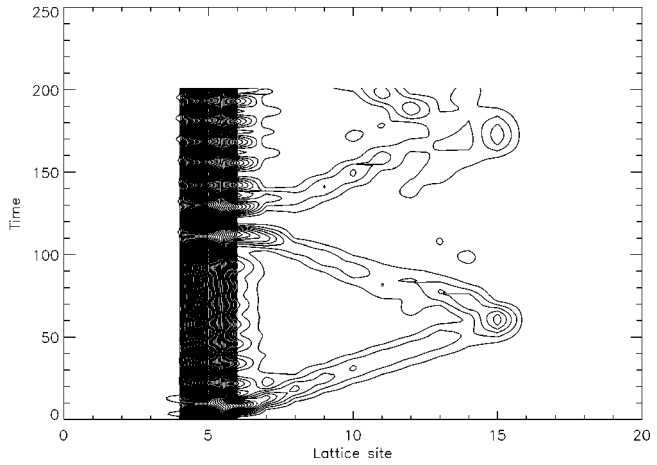

FIG. 9. Amplitude density plot for a donor–acceptor system separated by nine intermediate linear oscillators as a function of time. Energy is injected initially so that the resonance condition is fulfilled. We use $\lambda=0.1$; partial targeted energy transport is occurring.

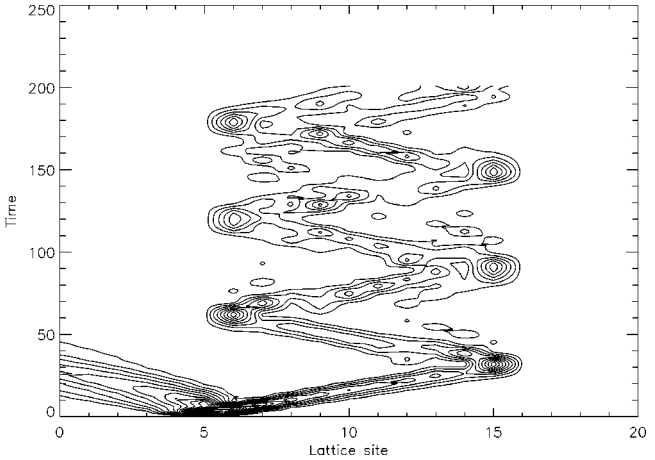

FIG. 10. Amplitude density plot for a donor–acceptor system separated by nine intermediate linear oscillators as a function of time. Energy is injected initially so that the resonance condition is fulfilled. We use $\lambda=0.2$; partial targeted energy transport is occurring.

VI. CONCLUSIONS

We close the selected summary of DB properties that we presented by departing from specific nonlinear models and discuss some less precise and more tentative ideas that are motivated, however, from the very nature of DB's as well as our interest to search for physical and especially biological realms for their utility. One difference that we observe between processes in physics and in biology is that the latter have evolved through competition and, as a result, ordinary minimization principles might be too simple to capture their complexity. Furthermore, the complex nature of the typically mesoscopic phenomena involved do not seem to permit the usual physics reductionist approach according to which an explanation and understanding is available at smaller length scales. One would be tempted to say that perhaps ''laws'' with the usual connotation we give to the word in physics are not as important in molecularly based biology as are ''mechanisms.'' We view a biological mechanism as a complex sequence of events involving chemical, configurational, energetic, entropic, etc., changes that are linked together and accomplish a certain function; the latter was developed in various biosystems in the course of evolution and contributes to organism fitness. An interesting example of such a mechanism is provided by protein motility. Motor proteins are nanomachines that rectify chemical energy from ATP hydrolysis into mechanical translational energy, enabling them to move along microtubules. Kinesin, a typical example of such proteins, has a dimeric structure with head extent approximately 4 nm and moves along microtubules with step size one α-β tubulin dimer equal to 8 nm.[27–30] In the process of its ''walk'' on the microtubule, kinesin consumes one ATP molecule per eight nanometer step. If we were to reduce the

walking mechanism into its more elementary processes we would identify the following: (i) Hydrolysis of ATP with energy deposition in a specific location of one of the kinesin heads (actually acting as ''legs'' rather than ''heads''); (ii) kinesin opening and translation of the other motor protein head; and (iii) movement of the first head to the new position and step completion. If this scenario of the motor protein walk is approximately correct, then energy localization must be invoked in the first two steps of the mechanism. For, in the first step, energy is deposited locally in some form while subsequently this energy can be thought as being funneled to a specific pivot site in the neck protein region and therefore enabling (ii). Discrete breather properties (iii) and (iv) can be linked together and provide both the means of motion for the initially localized energy as well as the specificity in the transfer. Similar ideas maybe invoked in principle in the rotary motors such as the F_1F_0 ATPase.[31]

The example of motor proteins is by no means unique as far as biological mechanisms involving in some stage localized energy. The best publicized case is amide-I vibrational energy localization and its connection to the ''Davydov soliton.'' [3] In the latter case a soliton or perhaps a polaron are formed due to self-trapping of carbon–oxygen vibrational stretching modes induced by strong coupling with other vibrational modes. It has been conjectured that this self-trapped state can propagate without losses and provide a mechanism for reliable energy transfer in some biomolecules. Although not conceived initially in this form, it could be possible that the Davydov soliton is actually some form of a discrete breather involving the amide-I vibration. In this case some of the properties of DB's reviewed could provide additional ideas and means for its experimental identification. In particular, the feature of slower statistical relaxation induced by persistent trapping in deep local minima of the biopolymer free energy landscape, may provide distinct signatures for nonlinear localization.[19] Discrete breathers appear to be quite versatile in managing localized energy. Once formed they can transport this energy efficiently by engaging the lattice in their motion. Furthermore, under specific circumstances they can transfer this energy in selected locations and thus introduce specificity. Fusing together precise facts from model studies as well some more general, extrapolative arguments, we see that breathers could in principle act as able energy managers in biomolecules; the real question of course is whether nature is actually using their services.

ACKNOWLEDGMENTS

This work has been partially supported by the European Union under Grants No. HPRN-CT-1999-00163 and No. HPMF-2002-01965.

[1] H. Frauenfelder, R. Austin, and P. G. Wolynes, Rev. Mod. Phys. **71**, S419 (1999).
[2] J. Onuchic, Z. Luthey-Schulten, and P. G. Wolynes, Annu. Rev. Phys. Chem. **48**, 545 (1997).
[3] A. C. Scott, Phys. Rep. **217**, 1 (1992).
[4] A. J. Sievers and S. Takeno, Phys. Rev. Lett. **61**, 970 (1988).
[5] R. S. MacKay and S. Aubry, Nonlinearity **7**, 1623 (1994).
[6] G. P. Tsironis and S. Aubry, Phys. Rev. Lett. **77**, 5225 (1996).
[7] A. Bikaki, N. K. Voulgarakis, S. Aubry, and G. P. Tsironis, Phys. Rev. E **59**, 1234 (1999).
[8] R. Roncaglia and G. P. Tsironis, Phys. Scr. **61**, 123 (2000).
[9] K. O. Rasmussen, S. Aubry, A. R. Bishop, and G. P. Tsironis, Eur. J. Phys. B **15**, 169 (2000).
[10] K. Y. Tsang and K. L. Ngai, Phys. Rev. E **54**, R3067 (1996).
[11] S. R. Bickham, S. A. Kiselev, and A. J. Sievers, Phys. Rev. B **47**, 14 206 (1993).
[12] T. Dauxois and M. Peyrard, Phys. Rev. Lett. **70**, 3935 (1993).
[13] D. Chen, S. Aubry, and G. P. Tsironis, Phys. Rev. Lett. **77**, 4776 (1996).
[14] S. Aubry, G. Kopidakis, A. M. Morgante, and G. P. Tsironis, Physica B **296**, 222 (2001).
[15] G. Kopidakis, S. Aubry, and G. P. Tsironis, Phys. Rev. Lett. **87**, 165501 (2001).
[16] J. L. Marin and S. Aubry, Nonlinearity **9**, 1501 (1996).
[17] S. Flach and C. R. Willis, Phys. Rep. **295**, 182 (1998).
[18] J. A. McCammon and M. Karplus, Annu. Rev. Phys. Chem. **31**, 29 (1980).
[19] A. Xie, L. VanderMeer, W. Hoff, and R. H. Austin, Phys. Rev. Lett. **84**, 5435 (2000).
[20] Y. S. Kivshar and M. Peyrard, Phys. Rev. A **46**, 3198 (1992).
[21] T. S. Rose, R. Righini, and M. D. Fayer, Chem. Phys. Lett. **106**, 13 (1984).
[22] V. M. Kenkre, in *Exciton Dynamics in Molecular Crystals and Aggregates*, Spinger Tracts of Modern Physics (Springer-Verlag, Berlin, 1982), Vol. 94.
[23] R. Reigada, M. Ibanes, J. M. Sancho, and G. P. Tsironis, J. Phys. A **34**, 8465 (2001).
[24] G. P. Tsironis, M. Ibanes, and J. M. Sancho, Europhys. Lett. **57**, 697 (2002).
[25] M. Ibanes, J. M. Sancho, and G. P. Tsironis, Phys. Rev. E **65**, 041902 (2002).
[26] X. Hu, A. Damjanovic, T. Ritz, and K. Schulten, Proc. Natl. Acad. Sci. U.S.A. **95**, 5935 (1998).
[27] M. J. Schnitzer and S. M. Block, Nature (London) **388**, 386 (1997).
[28] B. Tipet, R. D. Vale, and R. S. Hodges, J. Biol. Chem. **272**, 8946 (1997).
[29] W. Hua *et al.*, Nature (London) **388**, 390 (1997).
[30] G. Stratopoulos, T. E. Dialynas, and G. P. Tsironis, Phys. Lett. A **218**, 292 (1999).
[31] G. Oster, Nature (London) **417**, 25 (2002).
[32] G. P. Tsironis, Phys. Lett. A **173**, 381 (1993).
[33] J. C. Eilbeck, P. S. Lomdahl, and A. C. Scott, Physica D **16**, 318 (1985).
[34] V. M. Kenkre and D. K. Campbell, Phys. Rev. B **34**, 4959 (1986); V. M. Kenkre, G. P. Tsironis, and D. K. Campbell, in *Nonlinearity in Condensed Matter*, edited by A. R. Bishop *et al.* (Springer-Verlag, Berlin, 1987); G. P. Tsironis and V. M. Kenkre, Phys. Lett. A **127**, 209 (1988).